IOPscience iopscience.iop.org

Home Search Collections Journals About Contact us My IOPscience

Superconductivity in CVD diamond films

This article has been downloaded from IOPscience. Please scroll down to see the full text article.

2009 J. Phys.: Condens. Matter 21 253201

(http://iopscience.iop.org/0953-8984/21/25/253201)

View the table of contents for this issue, or go to the journal homepage for more

Download details:
IP Address: 129.252.86.83
The article was downloaded on 29/05/2010 at 20:14

Please note that terms and conditions apply.

J. Phys.: Condens. Matter **21** (2009) 253201 (11pp) doi:10.1088/0953-8984/21/25/253201

TOPICAL REVIEW

Superconductivity in CVD diamond films

Yoshihiko Takano

National Institute for Materials Science, 1-2-1 Sengen, Tsukuba 305-0047, Japan

Received 31 October 2007, in final form 10 March 2009
Published 27 May 2009
Online at stacks.iop.org/JPhysCM/21/253201

Abstract

A beautiful jewel of diamond is insulator. However, boron doping can induce semiconductive, metallic and superconducting properties in diamond. When the boron concentration is tuned over 3×10^{20} cm^{-3}, diamonds enter the metallic region and show superconductivity at low temperatures. The metal–insulator transition and superconductivity are analyzed using ARPES, XAS, NMR, IXS, transport and magnetic measurements and so on. This review elucidates the physical properties and mechanism of diamond superconductor as a special superconductivity that occurs in semiconductors.

(Some figures in this article are in colour only in the electronic version)

Contents

1. Introduction

Since the beginning of time people have been mesmerized by the glitter and beauty of diamond, the most precious stone of all. Even though diamonds were first mined in India as early as the 4th century BC, only during recent centuries has diamond become popular as a gemstone for jewelry. This is because special techniques are required for cutting and polishing diamond since it is a superhard material (the word diamond derives from the Greek 'adamas' meaning 'invincible'). In addition to its natural high hardness, diamond has an extraordinary range of material properties: diamond has the highest thermal conductivity at room temperature with a high Debye temperature [1]; it is an excellent electrical insulator; it is transparent to UV, visible, and IR radiation; it has a high refractive index; and it is physically and chemically stable. Furthermore, as a result diamond exhibits excellent internal reflection and refraction of light, which is the hallmark of the extraordinary brilliance, sparkle, and luster of cut diamonds.

In general, good thermal conductors, such as copper, are also good electrical conductors because of the available conduction electrons for the transfer of electrical current and heat. Surprisingly, diamond is an electrical insulator, yet exhibits high thermal conductivity. The high thermal conductivity of diamond is attributed to the high Debye temperature, that is, a high phonon frequency. It was speculated that the strong phonon frequency of diamond could be exploited to produce superconductivity; it was from this idea that the current research on superconductivity in diamond originated.

It is possible to search for a new superconductor by applying the McMillan relation, $T_C \approx \theta e^{(-(1+\lambda)/\lambda)}$, where λ is an electron–phonon interaction constant, since this relationship states that the superconducting transition temperature, T_C, is proportional to the Debye temperature θ [2]. Clearly, it is possible to identify many materials that exhibit a high Debye temperature, and thus there are many candidate materials. Among these materials is diamond, the most likely superconductor candidate with the highest Debye temperature. Unfortunately, diamond is an insulator with no charge carriers that can contribute to superconductivity; therefore, how can excess charge carriers be introduced into diamond?

Although pure diamond is an insulator with a 5.5 eV band gap, when doped with impurities such as trivalent boron (B)

 © 2009 IOP Publishing Ltd Printed in the UK

atoms, diamond exhibits p-type conductivity; the boron atoms replace the carbon site and form an impurity level with an activation energy of 0.37 eV. The doping process is similar to that used with silicon semiconductors. Blue diamonds, which contain boron impurities, are beautiful, expensive, and naturally occurring p-type semiconductors. However, when diamond is doped with nitrogen (N), phosphorus (P) or sulfur (S), the dopants act as donors, resulting in the formation of electron carriers, and the diamond exhibits n-type conductivity. Diamond semiconductors, with excellent properties such as high carrier mobility, are excellent materials for sensors, light emitting devices, and high-power/high-frequency devices. Nevertheless, because of the deep impurity level of boron (0.37 eV) and especially phosphorus (0.6 eV), the actual carrier density at room temperature is a few orders smaller than the dopant concentration, resulting in the low conductivity of devices [3]. There are also considerable barriers to overcome when mass producing diamond-based devices, because of the prohibitive cost of the material. If it were possible to produce diamond wafers several inches wide, at a low cost, the semiconductor industry, as well as jewelers, would witness a dramatic change.

2. High-pressure high-temperature (HPHT) synthesized diamond

Synthetic diamond is produced by two main methods: high-pressure high-temperature (HPHT) and chemical vapor deposition (CVD). The HPHT methods fall into two groups: direct conversion [4, 5] and industrial synthesis using a metal catalyst process (called the industrial process) [6–8]. Furthermore, in the direct conversion HPHT method graphite is subjected to conditions similar to those under which natural diamonds are formed; keeping pressures higher than 10 GPa, at temperatures around 3000 °C for several seconds in a small localized place, which make it difficult to produce large, single crystal diamonds. In contrast, the use of metal catalysts in the industrial process, which is performed at lower pressures and temperatures, produces large size, single crystal diamonds. During the industrial process the typical temperatures and pressures are 5–6 GPa and 1500 °C, respectively. Currently, almost all the diamonds used in the production of high strength cutting tools are synthesized using the industrial process. Due to the presence of nitrogen, the diamonds exhibit a yellow color and are categorized as type Ib.

In the spring of 2004, Ekimov *et al* [9] reported that boron-doped diamond samples synthesized using the HPHT method exhibit superconductivity with a resistive transition temperature of $T_C = 2.3$ K, at which the resistance drops to zero. Assuming the dirty limit of class II superconductors, they found that the upper critical field H_{C2} is 3.4 T, and thus calculated that the coherent length was about 10 nm. In addition, from the magnetization measurements the critical current density (J_C) was found to be 145 A cm^{-2}. This news was received with a great deal of surprise since diamond is considered to be an insulator.

Figure 1 is a schematic diagram of the high-pressure sample cell. The cell is stacked with alternating layers of graphite and B_4C, which is placed in a graphite heater. Using pressure equipment that employs the 'Troid' method, boron-doped diamond was synthesized at the boundary of graphite and B_4C under high-pressure and high-temperature conditions—typically the pressure and temperature were 10 GPa and 2200–2500 °C, respectively, similar to that in the direct conversion range. In the synthesis process, since the graphite heater is also converted into diamond, the heating time was approximately a few seconds. Unfortunately, it is difficult to synthesize large bulk or single crystal diamond samples because of the synthesis conditions and the short heating time [9–11].

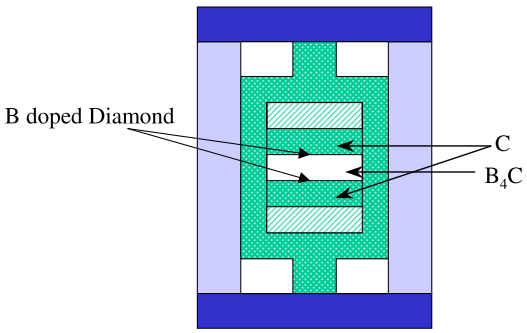

Figure 1. Schematic diagram of a sample cell for high-pressure synthesis.

There is the outstanding question of whether or not superconducting diamond can be synthesized using the industrial synthesis process, which can produce large diamond samples. Unfortunately, the answer up to now has been 'no'; due to an insufficient concentration of boron, superconducting diamonds have not yet been synthesized. This is attributed to the limited solid solubility of boron as a conventional metal catalyst. Further improvements in catalysts could lead to the production of superconducting diamond [12].

3. The chemical vapor deposition (CVD) method

The second method to produce synthetic diamond, chemical vapor deposition (CVD) using gases such as methane, was discovered in the 1980s [13, 14]; interestingly, at this time people were excited at the news that diamond could be grown from alcohol such as liquor! The hot filament CVD and the microwave plasma CVD methods were developed. Due to the incorporation of filament metals in the films deposited by a hot filament, the microwave plasma-assisted chemical vapor deposition (MPCVD) method was preferred. The sophisticated MPCVD apparatus using quartz tube piercing the waveguide was designed by Kamo *et al* [14]. Indeed the first superconducting diamond films were made by this Kamo-type apparatus [15]. The advantage of the CVD methods include the ability to grow large diamond thin films and diamond wafers, the finer control of impurities, and the wider range of the solid solubility limit. Clearly, this method contributed significantly to the development of diamond-based electronic devices. For the growth of boron-doped diamond films using the CVD method, boric gases such as diboran (B_2H_6) or trimethylboron

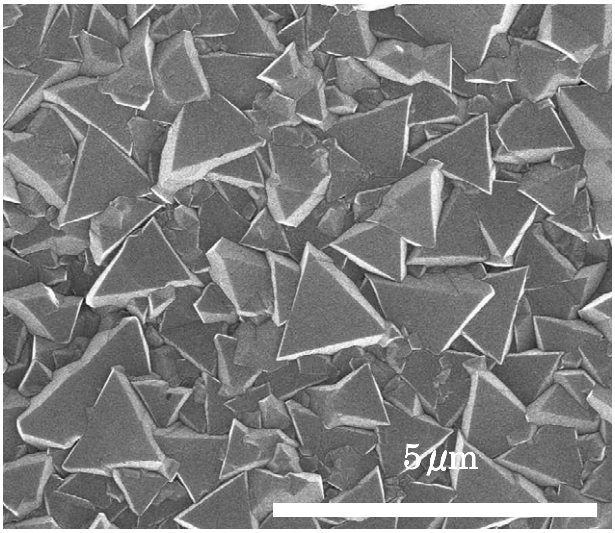

Figure 2. SEM image of a polycrystalline diamond thin film grown by CVD.

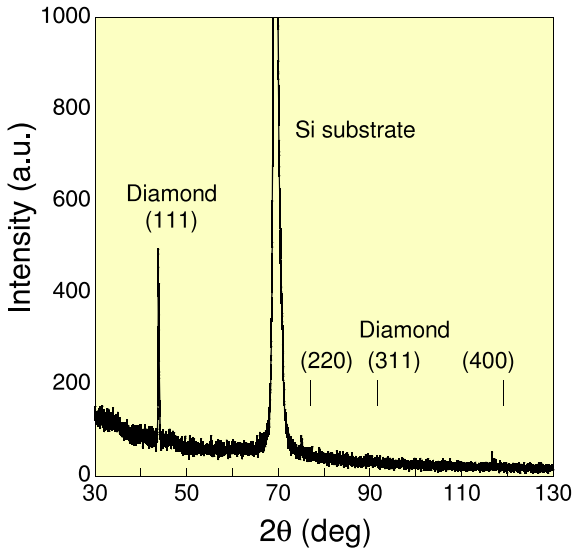

Figure 3. X-ray diffraction pattern of polycrystalline CVD diamond.

(TMB) were mainly used as the boron source. However, care must be exercised since diboran is a very toxic gas. Using these boric gases, it is possible that samples with a significant amount of doped boron can be simply produced using CVD; that is, it is possible to produce superconducting diamond samples.

4. Superconducting polycrystalline diamond films

Superconducting polycrystalline heavily boron-doped diamond films were successfully made using the MPCVD method [15, 16]. The deposition was carried out using a dilute gas mixture of methane (1–3%) and TMB in hydrogen. Changing the mixture ratio of methane and TMB is used to control the concentration of boron in the diamond samples. To introduce a lot of carrier into diamond films, a remarkably

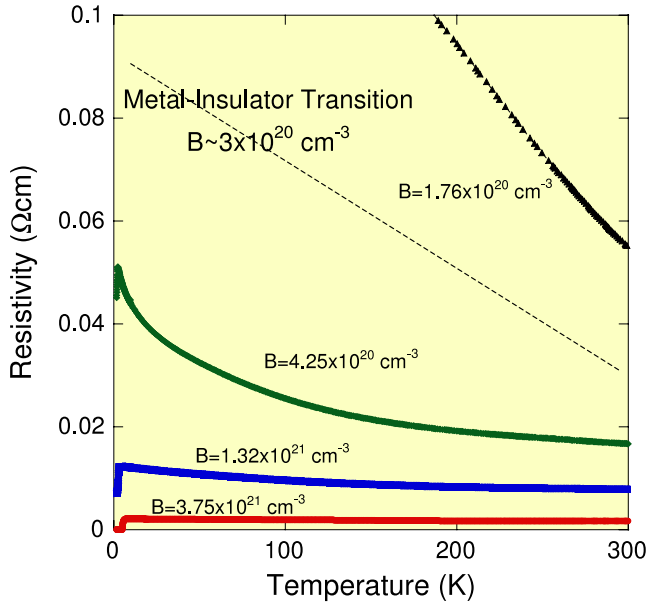

Figure 4. Temperature dependence of resistivity for diamond samples with different boron concentrations.

high boron to carbon (B/C) ratio of 1000–12 000 ppm was applied. Polycrystalline thin films were deposited on silicon substrates, which were pretreated by subjecting the samples to an ultrasonic bath of diamond powder (called the nucleation treatment). A scanning electron microscope (SEM) image of a polycrystalline diamond thin film grown using the CVD method on a (100) silicon substrate is presented in figure 2 [15, 16]. The film morphology consists of many triangular grains, so-called {111} facets, which suggests that the predominant growth orientation of the grains in the film is (111), which is confirmed from the x-ray diffraction (figure 3). In the x-ray diffraction pattern, assuming that the strongest peak corresponds to the Si substrate, only the peak corresponding to the (111) diamond thin film was detected at $2\theta = 43.9°$. No other peaks corresponding to (220), (311) and (400) were observed, and this indicates that the (111) growth orientation is dominant in boron-doped diamond, where the concentration of boron is high.

To observe the metal–insulator transition in diamond, the plot of the resistivity, as a function of temperature, for different boron concentrations is presented in figure 4; the concentration of boron was determined using a secondary ion mass spectrometer (SIMS). The sample with the lowest boron concentration ($N_B = 1.7 \times 10^{20}$ cm^{-3}) exhibits a high resistivity and is an insulator at low temperatures. The metal–insulator transition of diamond occurs at a boron concentration around $N_B = 3 \times 10^{20}$ cm^{-3} [16, 17]. For increasing boron concentration, the resistivity significantly decreases. Furthermore, the superconducting transition, corresponding to a sharp drop in resistivity, was also observed at low temperatures. For an increasing boron concentration, the superconducting transition temperature is also found to increase.

A further examination of the boron-doped sample with the highest concentration of boron revealed that the concentration of boron was an order of magnitude smaller than that found

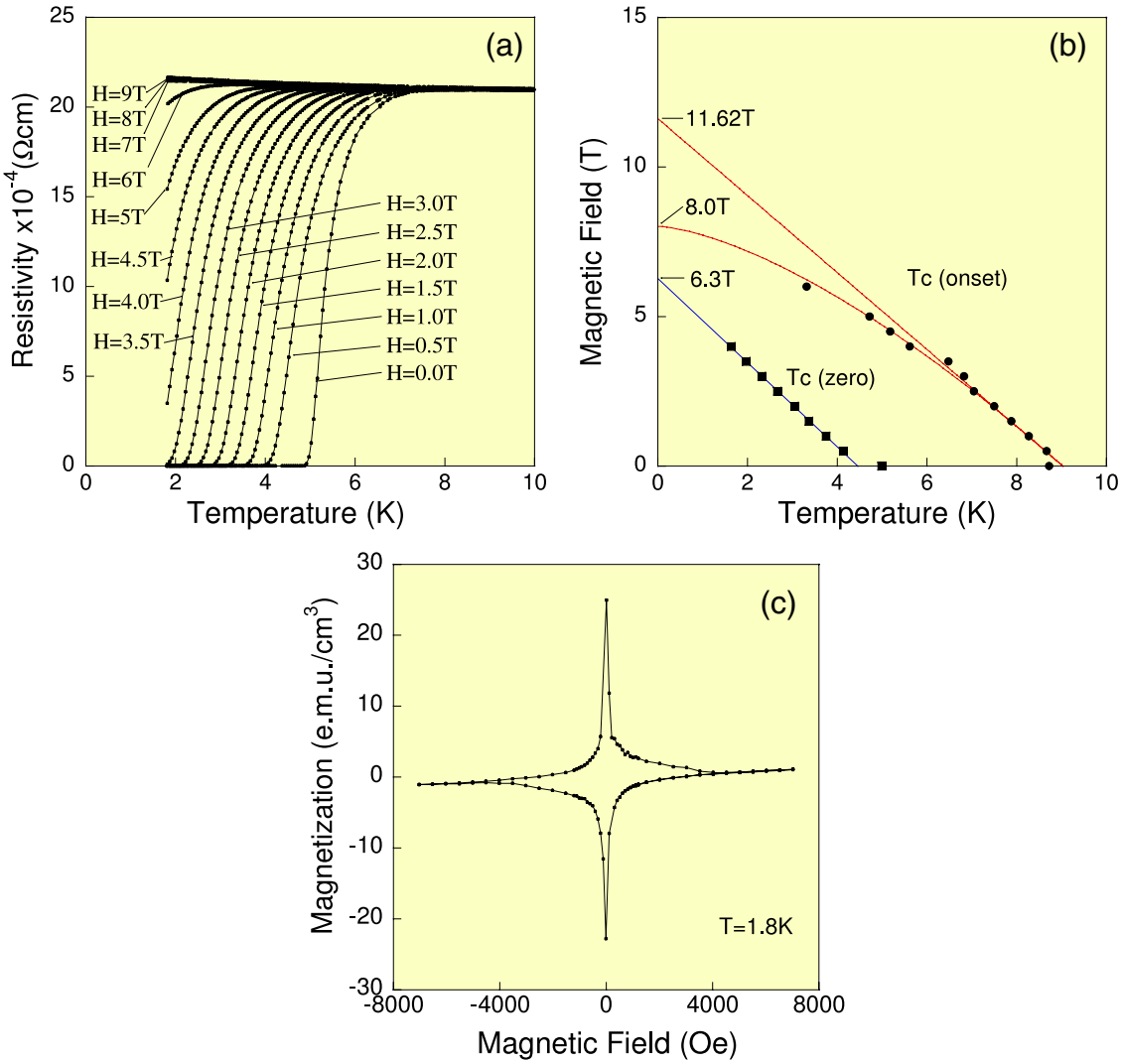

Figure 5. (a) Temperature dependence of resistivity under a magnetic field for polycrystalline diamond thin film. (b) The magnetic field dependence of T_C^{onset} and T_C^{zero} for polycrystalline diamond thin film. (c) Magnetization versus magnetic field (M–H) curvature of polycrystalline diamond thin film.

in high-T_C superconductors; where the concentration was $N_B = 3.75 \times 10^{21}$ cm^{-3}, which is equivalent to 2% of the B/C ratio. The temperature dependence of the resistivity for several values of the magnetic field is shown in figure 5(a). For zero magnetic field, the resistivity was found to drop at around 8.7 K (T_C^{onset}), and zero resistivity was obtained at 5.0 K (T_C^{zero}); the superconducting transition temperature was suppressed by the applied magnetic field. The field dependence of T_C^{onset} and T_C^{zero} is plotted as a function of temperature in figure 5(b). The linear extrapolation of T_C^{onset} and T_C^{zero} is used to determine the upper critical field (H_{C2}) and the irreversibility field, $H_{C2} = 11.62$ T, $H_{irr} = 6.3$ T, respectively. Assuming that the superconductivity in diamond is the dirty limit, the upper critical field H_{C2} is estimated to be about 8.0 T using the equation $H = H_{C2}^{WHH}(1 - T/T_C)^{1.5}$. We found that this equation shows good agreements with WHH theory, and the coherent length was determined as $\xi = 6.9$ nm using the equation $\xi = (\Phi_0/2\pi H_{C2})^{1/2}$ [1]. In the magnetization measurement, a diamagnetic response due to the Meissner effect was observed at approximately the zero resistivity temperature. The magnetization versus magnetic field (M–H) curve, which is a large symmetric hysteresis curve, highlights the typical characteristics of type-II superconductors (figure 5(c)). Based on the Bean model [18], the critical current density (J_C) was estimated as 500 A cm^{-2}, which is considerably higher than that for those samples prepared using the HPHT method. However, to produce a fine grain boundary the J_C level must be higher [9, 15, 16]. Moreover, a nanocrystalline boron-doped diamond thin film was also successfully grown using the CVD method and showed superconductivity in low-temperature transport measurements [19].

The correlation between the carrier concentration and the superconducting transition temperature was examined, where the carrier concentration was determined from Hall effect measurements. For an increasing carrier concentration the superconducting transition temperatures T_C^{onset} and T_C^{zero} were found to increase, suggesting that the samples were

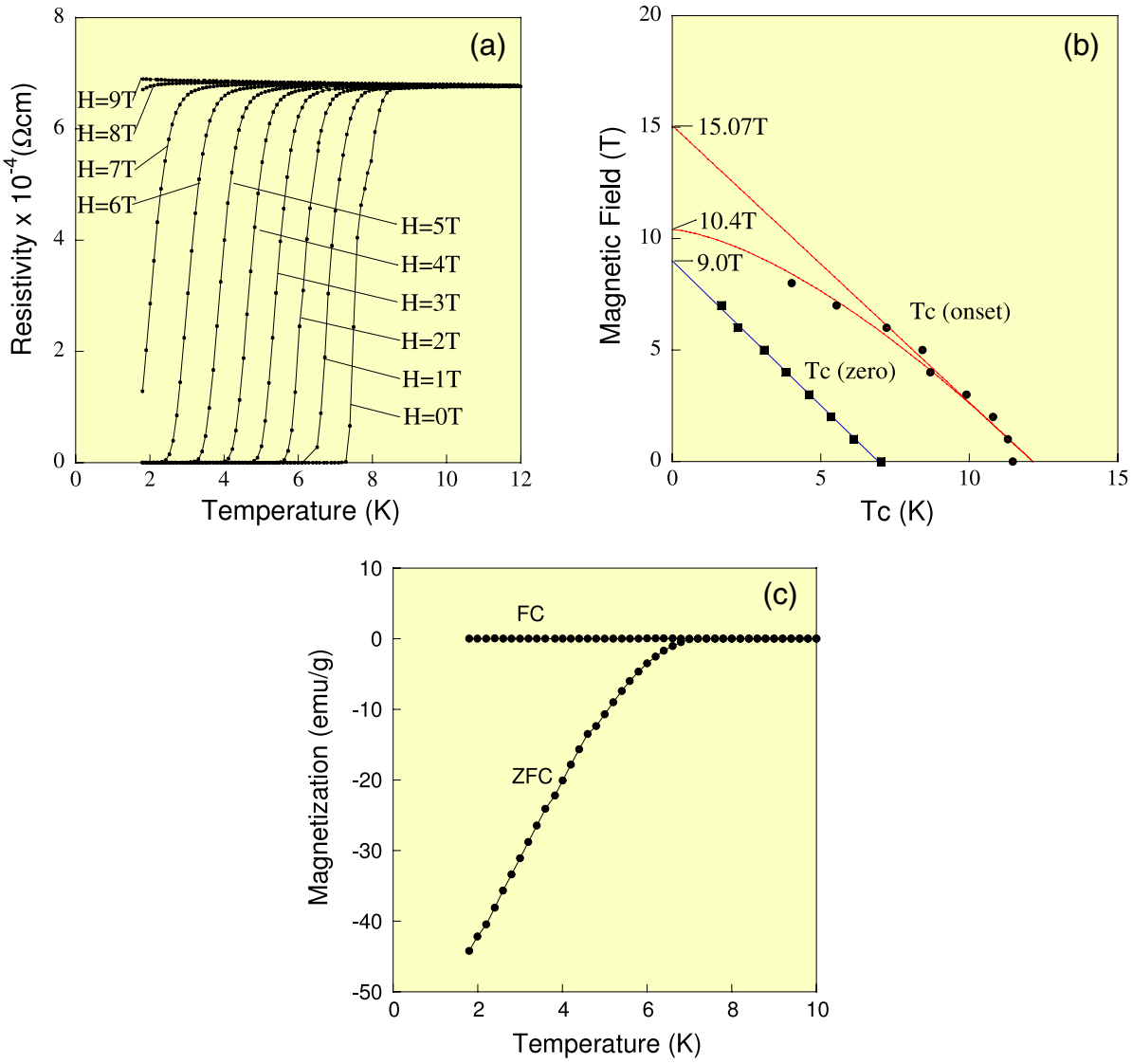

Figure 6. (a) Temperature dependence of resistivity under a magnetic field for homoepitaxial (111) diamond film. (b) The magnetic field dependence of T_C^{onset} and T_C^{zero}. (c) Temperature dependence of magnetization.

underdoped and the maximum T_C is assumed to be of a higher carrier concentration. For a much higher concentration, however, the carrier concentration calculated using the Hall effect measurements is found to be higher than the boron concentration determined from SIMS. This contradictory result requires further investigation of the electronic structure of the samples.

5. Superconducting homoepitaxial diamond films

Boron-doped homoepitaxial films were deposited on polished HPHT synthesized Ib single crystal diamond (111) and (100) substrates using the MPCVD method. The methane concentration in the growth conditions was 1–3% and the B/C ratio varied from 1000 to 12 000 ppm. In this section, the superconducting properties of homoepitaxial (111) film are mentioned first and the (100) film next.

Homoepitaxial (111) thin films with a boron concentration of 8.5×10^{21} cm^{-3}, corresponding to a B/C ratio of ∼5% and with a thickness of 2–3 μm, were obtained using a methane concentration of 3% in hydrogen and a B/C ratio of 6000 ppm using TMB as the boron source [20–23]. The resistance characteristics of the (111) films for a zero field condition, as a function of temperature, are plotted in figure 6. The resistivity above 8 K is 'flat', highlighting that there is no change with temperature in the normal conductivity state. At low temperatures, where superconductivity starts, the temperature at which the resistance starts to diverge from the normal-state resistance is defined as T_C^{onset} and the temperature of zero resistance is defined as T_C^{zero}. In the absence of a magnetic field (zero field cooling, ZFC), the superconducting transition temperatures of the (111) thin films were determined to be $T_C^{onset} = 11.4$ K and $T_C^{zero} = 7.4$ K; T_C^{onset} is clearly above 10 K which is also the case for T_C^{zero} if we take into consideration the affect of lower T_C due to grain boundaries in the thin film. To the best of our knowledge these values are the highest superconducting transition temperatures reported to date for superconducting diamonds. A temperature of 10 K can be

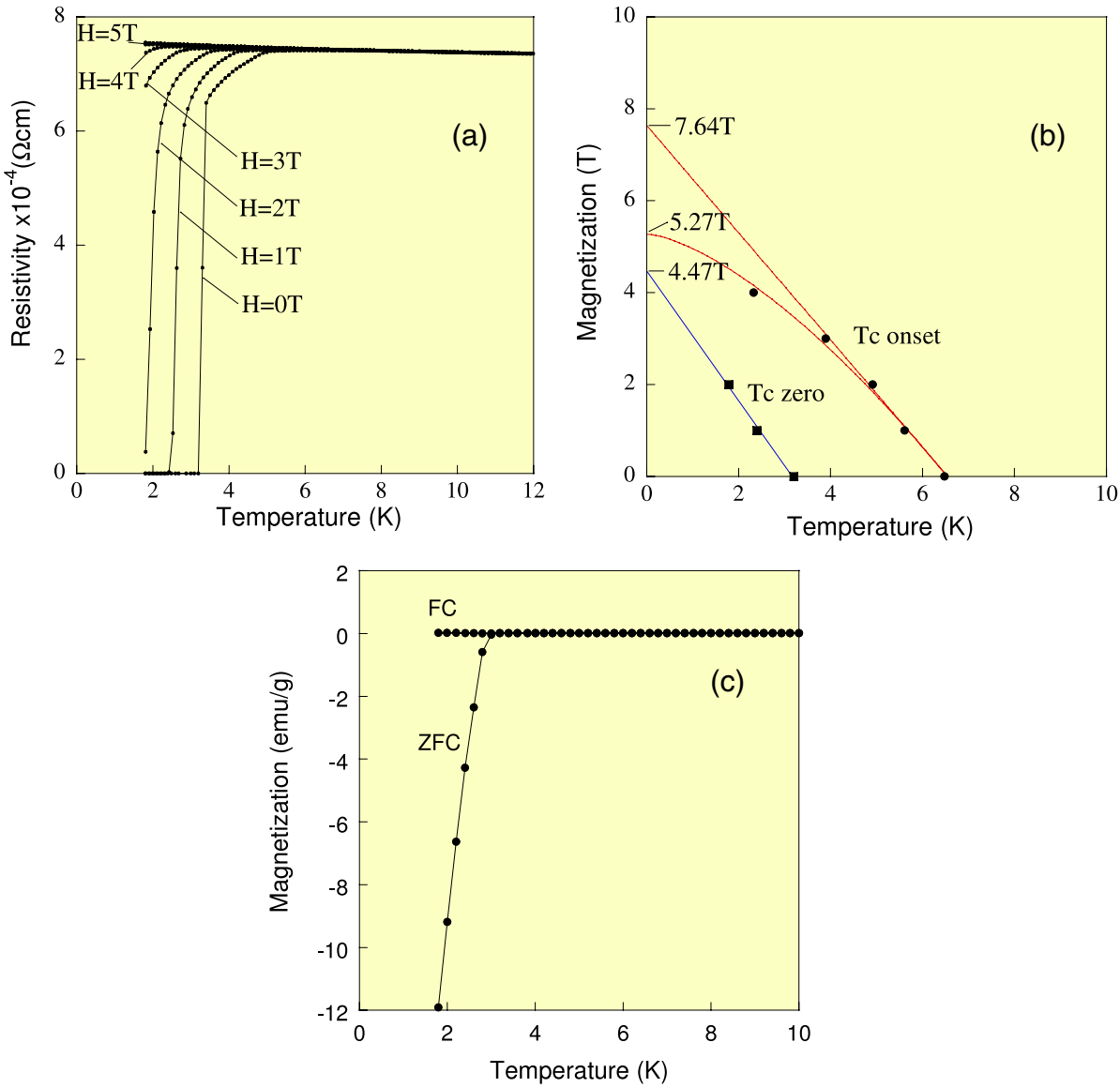

Figure 7. (a) Temperature dependence of resistivity under a magnetic field for homoepitaxial (100) diamond film. (b) The magnetic field dependence of T_C^{onset} and T_C^{zero}. (c) Temperature dependence of magnetization.

obtained easily using refrigeration equipment instead of costly liquid helium, which could have significant technological implications in the areas of fundamental and applied research. The superconducting transition temperature is shifted to lower temperatures for an increasing applied magnetic field. From the linear approximation of the field dependence of T_C^{onset} and T_C^{zero}, the upper critical field (H_{C2}) and the irreversible field (H_{irr}) are determined to be $H_{C2} = 15.07$ T and $H_{irr} = 9.0$ T, respectively (figure 6(b)). Assuming that the superconductivity is in the dirty limit, the upper critical field (H_{C2}) is estimated to be 10.4 T, for a coherent length of $\xi = 5.51$ nm. From the plots of the temperature dependence of the magnetization (figure 6(c)) at around the zero resistivity temperature of 7.4 K, diamagnetic signals are observed and are found to increase for decreasing temperature.

In contrast, for homoepitaxial (100) thin films with a boron concentration $N_B = 8.5 \times 10^{21}$ cm^{-3} deposited using the methane = 3% and B/C = 12 000 ppm, the superconducting transition temperatures are $T_C^{onset} = 6.3$ K and $T_C^{zero} = 3.2$ K, which are about half those obtained for the (111) thin films even at the same boron concentration as presented in figure 7(a). Similarly, from the field dependence on T_C^{onset} and T_C^{zero}, the upper critical field was estimated to be $H_{C2} = 7.64$ T (assuming the dirty limit, $H_{C2} = 5.3$ T) and $H_{irr} = 4.47$ T, and the coherent length $\xi = 7.89$ nm; these results indicate that the superconducting properties are significantly suppressed (figure 7(b)). The temperature dependence of the magnetization is illustrated in figure 7(c). Diamagnetic signals (the Meissner effect) were observed at approximately 3.2 K, where the resistivity drops to zero, and the ZFC curvature is found to decrease at lower temperatures [20–23]. The T_C dependence on boron concentration in the range of $N_B = 3.6$–19×10^{20} cm^{-3} was also studied using the (100) homoepitaxially deposited films with a methane concentration of 4% and B/C = 1500–3000 ppm [24]. T_C varied from 0 to 2.1 K, which is significantly lower than that of (111) films.

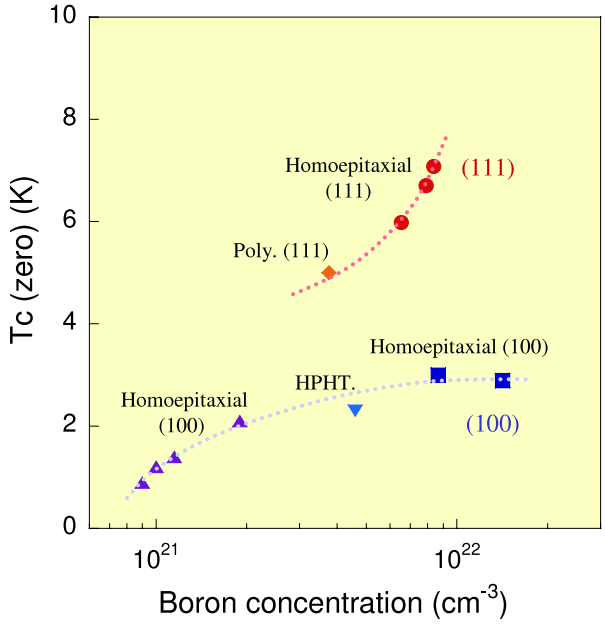

Figure 8. Superconducting transition temperature T_C^{zero} as a function of boron concentration.

The boron concentration dependence of T_C is summarized in section 6.

6. T_C dependence on boron concentration

In previous sections it was stated that the superconductivity in diamond thin films is strongly dependent on the crystal structure orientation of the films. The dependence of the superconducting transition temperature was evaluated using diamond thin films with different boron concentrations and substrate orientations. The correlation of the superconducting transition temperature (T_C^{zero}) with the concentration of boron is presented in figure 8 [9, 15, 16, 20–24]. It was observed that the superconducting transition temperature of the (111) single crystalline thin films significantly increases when the boron concentration is increased, which also corresponds to an increase in the carrier concentration. This is indicative of an under-doped state for high-T_C superconductors, which presents an interesting question; What is the optimum doping level for the (111) thin film?

In contrast, the superconducting transition temperature of the (100) single crystalline thin film, on the whole, is lower than that of the (111) film. In figure 8, the superconducting transition temperature exhibits a gradual increase for an increase in boron concentration. The transition temperature reaches a maximum at around $N_B = 10^{22}$ cm^{-3} and is not expected to be higher for further increases of boron. In the (100) thin films, boron does not result in carriers efficiently suppressing the occurrence of superconductivity. The HPHT synthesized diamond sample fits the (100) thin film curve; this property may suggest that the orientation of the HPHT synthesized film is the (100) direction, which may limit the superconducting transition temperature.

Table 1. Lattice expansions parallel/perpendicular to the film for (111) and (100) diamond films a–e.

	Lattice expansion				
Sample	a:(111) film	b:(111) film	c:(111) film	d:(100) film	e:(100) film
T_C^{zero} (K)	7.4	4.6	2.6	4.4	3.0
Perpendicular expansion (%)	0.48	0.44	0.44	0.51	0.46
In-plane expansion (%)	0.02	0.02	0.02	0.55	0.57

As mentioned, for the same boron concentration the (111) thin films exhibited high superconducting transition temperatures, while the superconducting properties in (100) films were significantly suppressed. Some possible causes, such as distortion of the crystal lattices and the concentration of effective doped boron, have been suggested [20, 21]. When doped with boron, the growth direction of the diamond crystal lattice is different in the (111) and (100) films. The results of the expansion rate of the crystal lattices parallel/perpendicular to the thin film for the sample are summarized in table 1. In the (111) thin films, the crystal lattices only expand perpendicular to the thin films and no in-plane expansion was observed, highlighting the distorted crystal lattice constant. In contrast, the crystal lattices of the (100) thin film exhibited isotropic expansion both in-plane and perpendicular to the thin film. These differences in the lattice distortions are assumed to give rise to the changes in the density of states, which may result in the different superconducting properties [20, 21].

Furthermore, two different states of boron in diamond have been determined from nuclear magnetic resonance (NMR) analysis and x-ray absorption spectroscopy (XAS) measurements: (1) a boron atom is substituted into the carbon diamond crystal lattice, (2) a boron atom accompanied by a hydrogen or boron atom is substituted into the carbon diamond crystal lattice [20, 21]. If a single boron atom is substituted into the diamond crystal lattice, a hole is introduced into the electronic band structure of the host diamond lattice. However, a boron–hydrogen/boron–boron pair, which is electro-neutral, does not result in the introduction of a hole in the energy band of diamond. Thus, compared to the apparent boron concentration, the effective boron concentration level required for carrier introduction is lower, where the ratio is in inverse proportion to the B–B and B–H pairs. From measurements using NMR, the effective 'isolated boron' concentration that is required to create carriers (holes) was determined; this value is in good agreement with the boron concentration $N_B = 1.9 \times 10^{21}$ cm^{-3} estimated from angle-resolved photoemission spectroscopy (ARPES) measurements, described in detail in section 8. Thus, to produce a diamond superconductor that exhibits good properties, the B–B and B–H pairs in diamond should be reduced [25–29].

7. Superconducting gap

Observations of the superconducting gap have been reported from spectrum measurements using laser-excited

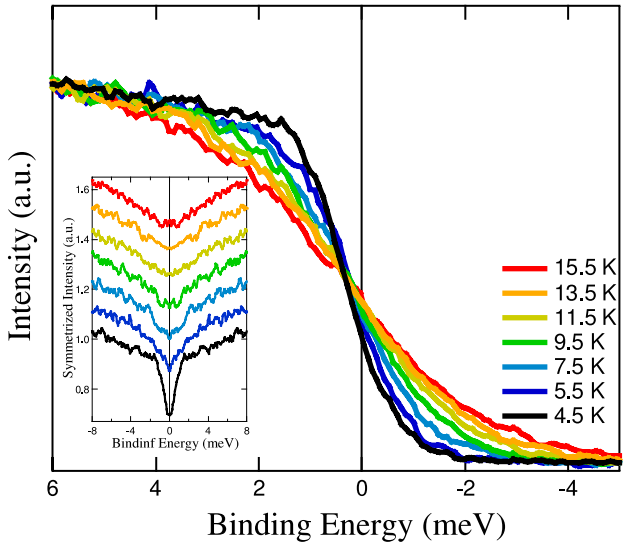

Figure 9. Superconducting gap observed by photoemission spectroscopy.

photoemission spectroscopy, sub-terahertz spectroscopy, and scanning tunneling spectroscopy (STS) [30–34].

Figure 9 is the photoemission spectrum (PES) of the superconducting state of a (111) diamond thin film observed using a laser with 6.994 eV. The superconducting gap was observed above 10 K and is consistent with the values of T_C^{onset} of the electric resistivity. The parameters obtained are $\Delta(4.5\ \mathrm{K}) = 0.78$ meV, $2\Delta(0)/k_B T_C^{mag} = 3.56$ ($T_C^{mag} = 6.6$ K), close to estimated typical values for weakly coupled BCS superconductors. A broad shape of the superconducting gap spectrum, with a broadening parameter of $\Gamma = 0.7$ meV, is a remarkably large value at a relatively higher temperature, indicative of some sort of disorder [30].

Homoepitaxial (111) thin films with a superconducting transition temperature of $T_C = 5.4$ K (determined from magnetization measurements) were measured using STS at 0.5 K. The spectrum is presented in figure 10(a), showing a clear superconductive gap. The parameters obtained from these measurements, $\Delta(0) = 0.87$ meV, and $2\Delta/k_B T_C = 3.7$, are close to the BCS values. The shape of the gap is broad, similar to that of PES, and the broadening parameter is $\Gamma = 0.38$ meV. These results are similar to those of granular superconductors and indicate a disorder induced because of the boron atoms [33].

On the other hand, for a (100) thin film with a low boron concentration of $N_B = 2.1$–3.1×10^{21} cm^{-3} and low superconducting transition temperature of 1.9 K, a typical s-wave superconducting gap was observed as shown in figure 10(b). The obtained parameter of $2\Delta/k_B T_C = 3.48$ suggests that the boron-doped diamond has characteristics of a BCS superconductor with weak coupling. However, the spatial vortex distribution is strongly disordered, demonstrating the existence of many pinning centers [34].

These differences in the spectral shape of the superconducting gap can be related to boron concentration and superconducting transition temperatures. STS measurements of (100) thin film with the same boron concentration as that of the (111) thin film will reveal the difference in the superconducting properties between the films, and the effect of the disorder induced because of the boron doping [35].

8. Metal–insulator transition of boron-doped diamond

To characterize better the mechanism of superconductivity in diamond, it is important to first characterize the electronic structure of the material. ARPES was performed using soft x-rays in the SPring-8 system, which is the large synchrotron radiation facility located in Hyogo prefecture in Japan [36, 37]. A photon energy of about 800 eV was used to perform measurements on diamond thin films with boron concentrations of $N_B = 8.37 \times 10^{21}$ cm^{-3}, $N_B = 1.18 \times 10^{21}$ cm^{-3}, and $N_B = 2.88 \times 10^{20}$ cm^{-3}. Band dispersions around the Γ point obtained from ARPES measurements are presented in figure 11. The white curves are the calculated energy band dispersion for pure diamond. The band structure of heavily boron-doped diamond is basically consistent with that of pure diamond. The diamond sample with the lowest boron concentration ($N_B = 2.88 \times 10^{20}$ cm^{-3}) did not exceed the metal–insulator transition level; the calculated band dispersion of this sample lies slightly below the Fermi level,

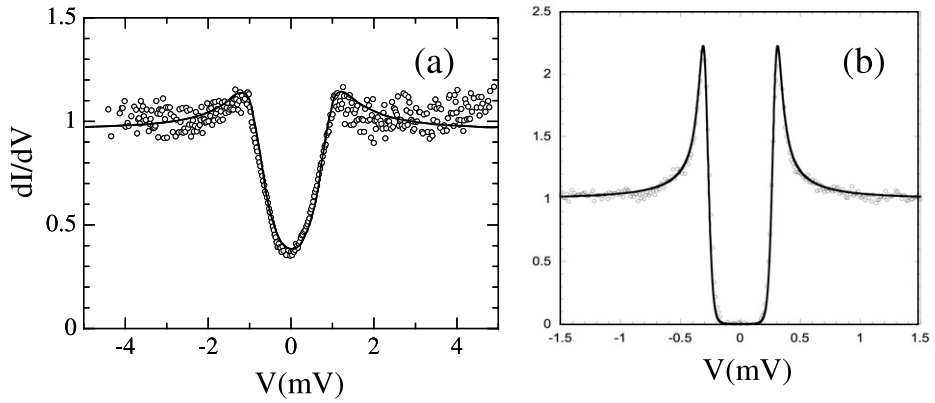

Figure 10. Superconducting gap observed by scanning tunneling spectroscopy for homoepitaxial (111) film (a) and (100) film (b).

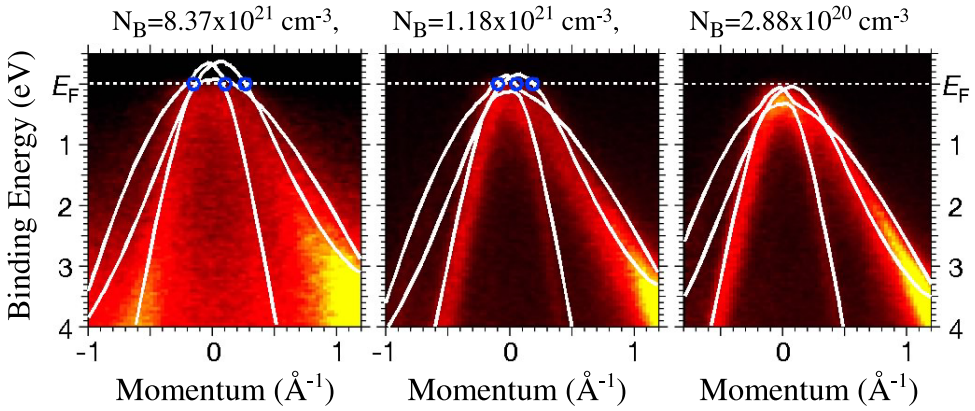

Figure 11. Soft x-ray angle-resolved photoemission spectroscopy (ARPES) of boron-doped diamond films.

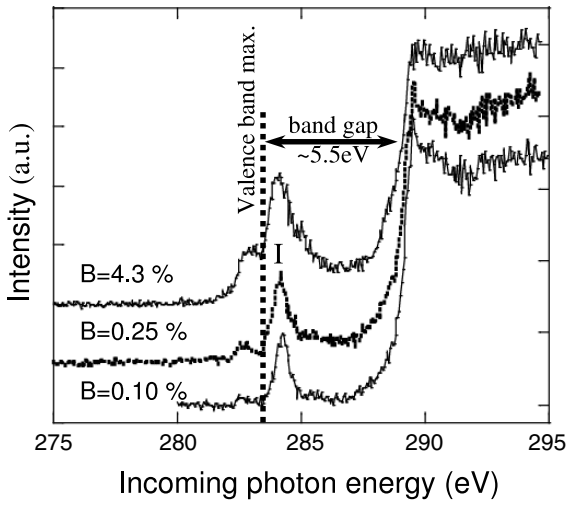

Figure 12. X-ray absorption spectra (XAS) of boron-doped diamond.

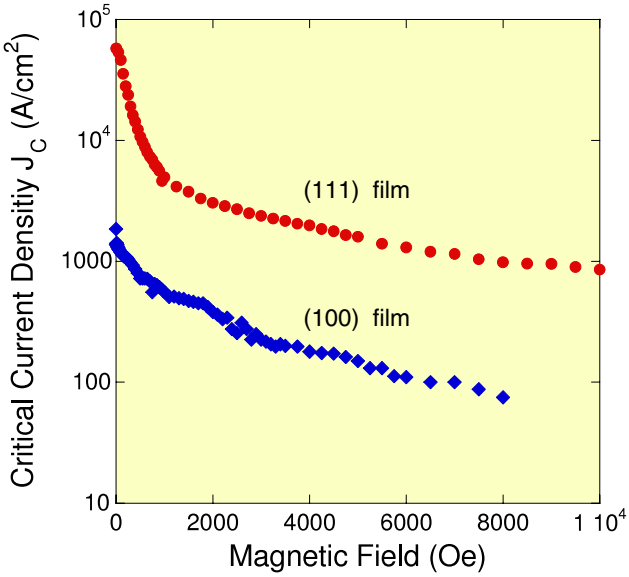

Figure 13. Critical current density J_C as a function of the magnetic field.

not representative of metallicity. For an increasing boron concentration, the energy bands of diamond shift toward the higher binding energy regions and are found to cross the Fermi level. These results indicate that the metallicity of the boron-doped diamond is due to the original band structure of the underlying diamond. If the heavily boron-doped diamond superconductors behave as 'conventional' superconductors, the superconductivity of the boron-doped material is assumed to be directly related to the energy band structure of diamond.

Figure 12 shows the x-ray absorption spectra (XAS) of the superconducting and non-superconducting diamond samples for different boron concentrations [26]. A 5.5 eV band gap is clearly observed between the valence and conduction bands. Peak I, which is located above the top of the valence band, is consistent with a boron acceptor level of 0.37 eV, which is suggestive of an impurity level of boron. Baskaran was the first to propose superconductivity because of the boron–impurity band, based on the resonating valence band (RVB) theory [38, 39]. The crossover from the superconductivity in the host band to that in the impurity band is investigated for the understanding of superconductivity in doped semiconductors [40, 41].

The dispersion of the optical phonons in samples were measured using inelastic x-ray scattering (IXS) [42, 43]. For the measurements, heteroepitaxial boron-doped diamond thick films were prepared using the CVD method, in which the substrates were etched away after growth. The longitudinal optical (LO) phonons were found to be softened by as much as ∼8 meV near the Γ-point, where the softening is suppressed toward the zone-boundary point L. This suggests that strong electron–phonon interactions contribute to the superconductivity in diamond. Although in some publications [44–51] it is highlighted that superconductivity in diamond is explained by the BCS theory, the softening rate of the optical phonons predicted from the virtual crystal approximation (VCA) is much higher than experimental values. It is also found that the softening of the optical phonons, determined from *ab initio* pseudopotential calculations using a 10 × 10 × 10 supercell, is in good agreement with the experimental result [48]. Many parameters characterized from experiments will be employed to develop the existing theories further.

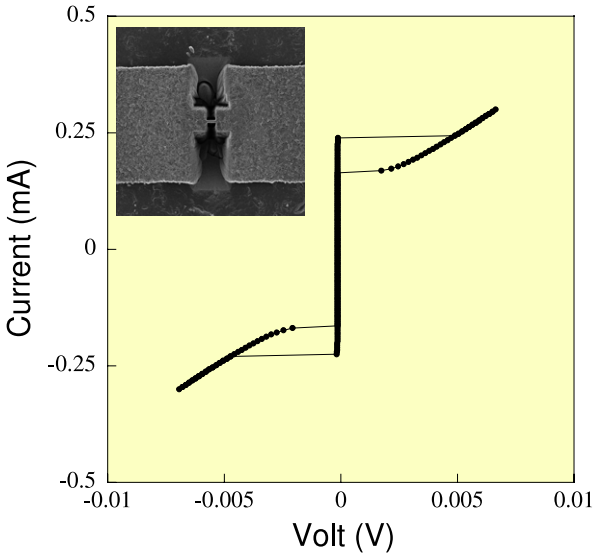

Figure 14. Current–voltage (I–V) characteristics of a grain boundary junction. Inset: SIM image of a Josephson junction fabricated using FIB.

9. Critical current density and Josephson junction

The critical current density (J_C) of homoepitaxial (111) and (100) diamond thin films, with nanofabricated thin wires and four terminals, was measured using the applied current method. The critical current density as a function of the magnetic field is plotted in figure 13. For the (111) thin film, J_C for a zero magnetic field was 57 500 A cm^{-2}, which is two orders of magnitude higher than that of diamond polycrystalline thin films. This indicates that single crystalline substrates exhibit good crystal in-plane orientations and fine grain boundary connectivity, leading to such a high J_C. When a magnetic field was applied, however, around 0.1 T, the J_C initially drops then gradually decreases. For the (100) thin film, for which the superconducting transition temperature is low, J_C was found to be 1633 A cm^{-2}, which is relatively low. With an applied magnetic field, the J_C gradually decreases in contrast to the (111) thin film; What causes a high J_C in the (111) thin films at lower magnetic fields? In the (111) thin films, in general, columnar crystals tend to grow, while in the (100) thin films in-plane growth is usual. The high J_C value observed for the (111) thin film at lower magnetic fields can be due to pinning between the columnar crystal grains.

As mentioned above, J_C for the polycrystalline thin films is 500 A cm^{-2}, which is significantly lower than that of homoepitaxial thin films. Randomly oriented crystal grains in the plane of the thin films are assumed to give rise to such weak grain boundary connectivity. Can we take advantage of this weak connectivity to produce Josephson junctions? In this study a narrow bridge 1 μm in width was fabricated in a sample to include a single grain boundary, using a focused ion beam (FIB) etching machine. In figure 14, a SIM image of the fabricated sample (inset) and the measured I–V characteristics are presented, where the I–V characteristics include hysteresis is typical of a SIS (superconductor–insulator–superconductor) Josephson junction. Using the characteristics of the grain boundary, integrated semiconductor–superconductor based novel devices could be fabricated in the future.

10. Summaries and conclusions

Superconductivity observed in diamond is a rare form of superconductivity that is seen in typical band gap semiconductors [52, 53]. Boron-doped diamond is a p-type wide gap semiconductor. When a significant amount of boron is incorporated in the diamond lattice over $N_B = 3 \times 10^{20}$ cm^{-3}, diamond becomes metallic. ARPES suggested that the origin of metallicity is the holes in the diamond valence band. Superconductivity is achieved at a boron concentration above MIT, and T_C increases with increasing boron concentration. However T_C in homoepitaxial (111) film is significantly higher than that of (100) film even at the same boron concentration. The difference in T_C may depend on the effective carriers, which are introduced by an isolated boron substituted carbon site. On the other hand, B–B pairs and the B–H complex may not introduce any carriers in the diamond band. However, the doped boron introduces disorders. These disorders are assumed to suppress superconductivity. In recent years, theoreticians have predicted that it is possible to reach a remarkably high superconducting transition temperature if these disorders are removed. The Josephson junction was demonstrated using polycrystalline film. The development of new devices combining superconductivity and semiconductivity is anticipated.

Carbon, is an element unlike many others, that is found to be a building block for a broad variety of structures; for example diamond, graphite, fullerene C_{60}, amorphous carbon, etc. In diamond the atomic level structure exhibits three-dimensional sp^3-bonded carbon, which is in contrast to the two-dimensional sp^2-bonded structure found in graphite; the fullerene C_{60}, amorphous carbon and carbon nanotubes exhibit intermediate sp^2 and sp^3 bonding. As mentioned, superconductivity is observed in both diamond and graphite with a critical temperature around 12 K. In particular fullerene C_{60} exhibits the highest superconducting transition temperature among them. Although there is still no evidence for superconductivity in carbon nanotubes, it is believed that it is only a matter of time before superconductivity is demonstrated in carbon nanotubes; the superconducting behavior of a carbon nanotube is directly related to the one-dimensional nature of the nanotube. Clearly, compounds comprising carbon are of great interest in the field of superconductivity research.

Acknowledgments

The author would like to thank Dr H Kawarada and his students Mr T Takenouchi, Mr K Kobayashi, Mr S Tezuka, Mr S Iriyama, Mr R Okada, Mr T Ishiwata and Dr H Umezawa (currently at Advanced Industrial Science and Technology) of Waseda University for the valuable thin film production, including structural analysis and thin film fabrication. The author would also like to acknowledge the contribution of

our many colleagues in collaborative research: Dr T Yokoya and his group members in Okayama University for soft x-ray angle-resolved photoemission spectroscopy measurements, Dr K Ishizaka and Dr S Shin of the ISSP, University of Tokyo, for laser photoemission spectroscopy, Dr T Nishizaki IMR, Tohoku University, for STS spectra, Dr H Nakamura and Dr N Yamada of the University of Electro-Communications for x-ray absorption spectroscopy, Dr H Mukuda and Dr Y Kitaoka, Osaka University, for NMR measurements, Dr M Hoesch and Dr J Mizuki, SPring8, for IXS measurements, Dr I Sakaguchi of the National Institute of Materials for Science (NIMS) for SIMS measurements, Ms R Yamashita of NIMS for English translation, Dr M Nagao of NIMS for the measurements of the superconducting properties of diamond samples, and Mr T Okutsu, Mr S Ogawara, Mr T Watanabe, Mr K Deguchi, Mr Y Mizuguchi, Dr Y Kubo, Dr F Tomioka, Dr S Ueda, Dr S Ishii, Dr S Tsuda and Dr T Yamaguchi of our Nano Frontier Materials Group at NIMS for supporting this research.

References

[1] Tachiki M and Fujita T 1999 *Science of High Temperature Superconductivity* (Tokyo: Shokabo)
[2] MacMillan W L 1968 *Phys. Rev.* **167** 331
[3] Nebel C E and Ristein J 2003 *Thin-Film Diamond I* (*Semiconductors and Semimetals* vol 76) (New York: Elsevier)
[4] DeCarli P S and Jamieson J C 1961 *Science* **133** 1821
[5] Bundy F P 1962 *Science* **137** 1057
[6] Bundy F P, Hall H T, Strong H M and Wentorf R H Jr 1955 *Nature* **176** 51–5
[7] Bovenkerk H P, Bundy F P, Chrenko R M, Codella P J, Strong H M and Wentorf R H Jr 1993 *Nature* **365** 19
[8] Bovenkerk H B, Bundy F P, Hall H T, Strong H M and Wentorf R H Jr 1959 *Nature* **184** 1094–8
[9] Ekimov E A *et al* 2004 *Nature* **428** 542
[10] Ekimova E A, Sidorov V A, Rakhmanina A V, Mel'nik N N, Sadykov R A and Thompson J D 2006 *Sci. Technol. Adv. Mater.* **7** S2–6
[11] Dubrovinskaia N, Eska G, Sheshin G A and Braun H 2006 *J. Appl. Phys.* **99** 033903
[12] Kanda H and Sumiya H 2007 *New Diamond Front. Carbon Technol.* **17** (See this special issue and its references)
[13] Spitsyn B V, Builov L L and Deryagin B V 1981 *J. Cryst. Growth* **52** 219
[14] Kamo M, Sato Y, Matsumoto S and Setaka N 1983 *J. Cryst. Growth* **62** 642
[15] Takano Y, Nagao M, Sakaguchi I, Tachiki M, Hatano T, Kobayashi K, Umezawa H and Kawarada H 2004 *Appl. Phys. Lett.* **85** 2851
[16] Takano Y, Nagao M, Takenouchi T, Umezawa H, Sakaguchi I, Tachiki M and Kawarada H 2005 *Diamond Relat. Mater.* **14** 1936
[17] Thonke K 2003 *Semicond. Sci. Technol.* **18** S20–6
[18] Beam C P 1962 *Phys. Rev. Lett.* **8** 250
[19] Nesládek M, Tromson D, Mer C, Bergonzo P, Hubik P and Mares J J 2006 *Appl. Phys. Lett.* **88** 232111
[20] Takano Y, Takenouchi T, Ishii S, Ueda S, Okutsu T, Sakaguchi I, Umezawa H, Kawarada H and Tachiki M 2007 *Diamond Relat. Mater.* **16** 911
[21] Takano Y 2006 *Solid State Phys. (Kotaibutsuri)* **41** 457
[22] Umezawa H *et al* 2005 arXiv:cond-mat/0503303
[23] Umezawa H, Takenouchi T, Kobayashi K, Takano Y, Nagao M, Tachiki M, Hatano T and Kawarada H 2007 *New Diamond Front. Carbon Technol.* **17** 1
[24] Bustarret E 2004 *Phys. Rev. Lett.* **93** 237005
[25] Mukuda H, Tsuchida T, Harada A, Kitaoka Y, Takenouchi T, Takano Y, Nagao M, Sakaguchi I and Kawarada H 2006 *Sci. Technol. Adv. Mater.* **7** S37
[26] Nakamura J *et al* 2008 *J. Phys. Soc. Japan* **77** 054711
[27] Murakami M, Shimizu T, Tansho M, Takano Y, Ishii S, Ekimov E, Sidorov V, Kawarada H and Takegoshi K 2007 *Japan. J. Appl. Phys.* **46** L1138
Murakami M *et al* 2008 *Sci. Technol. Adv. Mater.* **9** 044103
[28] Yokoya T *et al* 2006 *Sci. Technol. Adv. Mater.* **7** S12
[29] Oguchi T 2008 *Sci. Technol. Adv. Mater.* **9** 044211
[30] Ishizaka K *et al* 2007 *Phys. Rev. Lett.* **98** 047003
[31] Ishizaka K *et al* 2006 *Sci. Technol. Adv. Mater.* **7** S17
[32] Ortolani M, Lupi S, Baldassarre L, Schade U, Calvani P, Takano Y, Nagao M, Takenouchi T and Kawarada H 2006 *Phys. Rev. Lett.* **97** 097002
[33] Nishizaki T, Takano Y, Nagao M, Takenouchi T, Kawarada H and Kobayashi N 2006 *Sci. Technol. Adv. Mater.* **7** S22
[34] Sace'pe' B, Chapelier C, Marcenat C, Kačmarčik J, Klein T, Bernard M and Bustarret E 2006 *Phys. Rev. Lett.* **96** 097006
[35] Shirakawa T, Horiuchi S, Ohta Y and Fukuyama H 2007 *J. Phys. Soc. Japan* **76** 014711
[36] Yokoya T, Nakamura T, Matsushita T, Muro T, Takano Y, Nagao M, Takenouchi T, Kawarada H and Oguchi T 2005 *Nature* **438** 647
[37] Yokoya T *et al* 2007 *New Diamond Front. Carbon Technol.* **17** 11
[38] Baskaran G 2008 *J. Supercond. Nov. Magn.* **21** 41
[39] Baskaran G 2006 *Sci. Technol. Adv. Mater.* **7** S49
[40] Yanase Y and Yorozu N 2008 *Sci. Technol. Adv. Mater.* **9** 044201
[41] Muranaka T, Kikuchi Y, Yoshizawa T, Shirakawa N and Akimitsu J 2008 *Sci. Technol. Adv. Mater.* **9** 044204
[42] Hoesch M, Fukuda T, Mizuki J, Takenouchi T, Kawarada H, Sutter J P, Tsutsui S, Baron A Q R, Nagao M and Takano Y 2007 *Phys. Rev.* B **75** 140508R
[43] Hoesch M, Fukuda b, T, Takenouchi T, Sutter J P, Tsutsui S, Baron A Q R, Nagao M, Takano Y, Kawarada H and Mizuki J 2006 *Sci. Technol. Adv. Mater.* **7** S31
[44] Boeri L, Kortus J and Andersen O K 2004 *Phys. Rev. Lett.* **93** 237002
[45] Boeri L, Kortus J and Andersen O K 2006 *Sci. Technol. Adv. Mater.* **7** S54
[46] Lee K W and Picket W E 2004 *Phys. Rev. Lett.* **93** 237003
[47] Blase X, Adessi Ch and Conne'table D 2004 *Phys. Rev. Lett.* **93** 237004
[48] Xiang H J, Li Z, Yang J, Hou J G and Zhu Q 2004 *Phys. Rev.* B **70** 212504
[49] Lee K-W and Pickett W E 2006 *Phys. Rev.* B **73** 075105
[50] Cardona M 2005 *Solid State Commun.* **133** 3–18
[51] Cardona M 2006 *Sci. Technol. Adv. Mater.* **7** S60
[52] Takano Y 2006 *Sci. Technol. Adv. Mater.* **7** S1 (Please see this special issue)
[53] Takano Y 2008 *Sci. Technol. Adv. Mater.* **9** 040301 (Please see this special issue)